



INTERNATIONAL ATOMIC ENERGY AGENCY

INDC(ITY)-012
Distr. G

I N D C INTERNATIONAL NUCLEAR DATA COMMITTEE

**Activity Report of the ENEA Nuclear Data Project
in the Year 2004**

Prepared by

Alberto Ventura
Centro di Ricerche Ezio Clementel
Via Martiri di Monte Sole 4
40129 Bologna, ITALY

March 2005

IAEA NUCLEAR DATA SECTION, WAGRAMER STRASSE 5, A-1400 VIENNA

INDC documents may be downloaded in electronic form from http://www-nds.iaea.org/at/indc_sel.html or sent as an e-mail attachment. Requests for hardcopy or e-mail transmittal should be directed to services@iaea.org or to:

Nuclear Data Section
International Atomic Energy Agency
PO Box 100
Wagramer Strasse 5
A-1400 Vienna
Austria

Produced by the IAEA in Austria

March 2005

Activity Report of the ENEA Nuclear Data Project in the Year 2004

Prepared by

Alberto Ventura
Centro di Ricerche Ezio Clementel
Via Martiri di Monte Sole 4
40129 Bologna, ITALY

Abstract

The nuclear data activities at the Bologna Research Centre of the Italian National Agency for New Technologies, Energy and the Environment (ENEA) are described for the year 2004. All work was undertaken within the P9H6 project of the Division for Advanced Physics Technologies.

March 2005

TABLE OF CONTENTS

General Quantum Mechanics	7
Nuclear Structure Theory	8
Nuclear Reaction Theory and Experiments	10
Nuclear Data Processing and Validation.....	15
Computer Codes	17
Publications	21
Project Staff.....	24
Visiting Scientists.....	24

General Quantum Mechanics

Non-Hermitian quantum mechanics has played a key role in nuclear physics since the introduction of the optical model in reaction theory. It is of basic interest to investigate the properties of non-Hermitian Hamiltonians, \mathbf{H} , possessing either space-time, or dynamical symmetries, or both.

Our research has been focused on pseudo-Hermitian Hamiltonians, satisfying the intertwining relation $\mathbf{H}^\dagger = \boldsymbol{\eta} \mathbf{H} \boldsymbol{\eta}^{-1}$, where $\boldsymbol{\eta}$ is a Hermitian operator, not necessarily positive. Hermitian quantum mechanics is recovered in the trivial case $\boldsymbol{\eta} = \mathbf{1}$, while the choice $\boldsymbol{\eta} = \mathbf{P}$, with \mathbf{P} the parity operator, gives rise to \mathbf{PT} -symmetric quantum mechanics, where the Hamiltonian is neither invariant under parity transformation, \mathbf{P} , nor time reversal, \mathbf{T} , but is invariant under their product, \mathbf{PT} .

In the simplest case of one-dimensional Hamiltonian with a local potential, $\mathbf{H} = -\mathbf{d}^2/\mathbf{d}\mathbf{x}^2 + \mathbf{V}(\mathbf{x})$, \mathbf{PT} symmetry is equivalent to the following condition on the potential, $\mathbf{V}(\mathbf{x}) = \mathbf{V}^*(-\mathbf{x})$, *i. e.* the real part of \mathbf{V} is even, $\mathbf{V}_R(\mathbf{x}) = \mathbf{V}_R(-\mathbf{x})$ and the imaginary part is odd, $\mathbf{V}_I(\mathbf{x}) = -\mathbf{V}_I(-\mathbf{x})$. An interesting consequence of \mathbf{PT} symmetry is that the bound-state spectrum is real, if \mathbf{PT} is an exact symmetry, *i. e.* not only \mathbf{H} is \mathbf{PT} -invariant, but its eigenstates are also eigenstates of \mathbf{PT} , while the eigenvalues of \mathbf{H} come in complex conjugate pairs when \mathbf{PT} symmetry is spontaneously broken.

Other interesting properties of \mathbf{H} appear when, in addition to the space-time \mathbf{PT} symmetry, \mathbf{H} possesses also a dynamical symmetry, *i. e.* , for some specific choice of \mathbf{V} , \mathbf{H} is a function of the Casimir invariant of a Lie algebra: the case we have studied in detail is the \mathbf{PT} -symmetric version of the hyperbolic Scarf potential, with the pseudo-orthogonal algebra $\mathfrak{so}(2,2)$ as the underlying dynamical symmetry [A.1].

Moreover, we have undertaken a systematic survey of scattering in one-dimensional \mathbf{PT} -symmetric mechanics, with particular reference to the relations connecting transmission coefficients and reflection coefficients for incident waves travelling from left to right and from right to left and derived them in detail for some local and non-local solvable potentials.

Structure of the odd-odd nucleus ^{134}Pr

Continuing a long-standing tradition in the development and application of algebraic models of nuclear structure, the interacting boson fermion-fermion model (IBFFM) of odd-odd nuclei has been employed in the analysis of the positive-parity doublet bands in ^{134}Pr [A.2]: Figure 1 shows a comparison of experimental and calculated energy spectra.

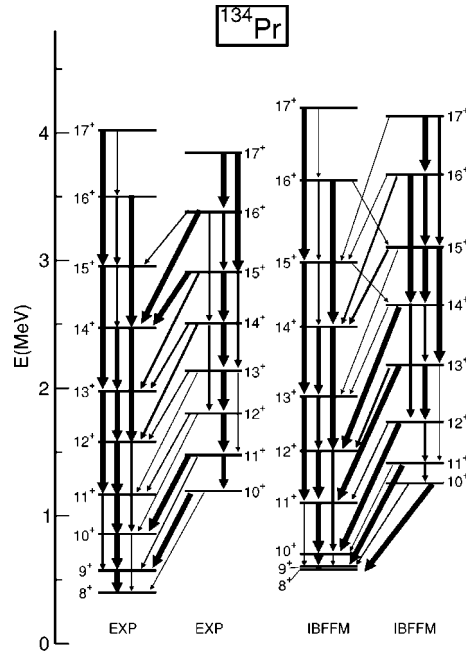


Fig. 1. Comparison of the experimental doublet of nearly degenerate positive-parity bands in ^{134}Pr with the lowest two bands calculated in the IBFFM. The calculation includes the triaxial deformation of the core. The thickness of the arrows that denote transitions corresponds to the relative gamma intensity in each branch.

In particular, it has been shown that stable triaxial deformation gives rise to the experimentally observed crossing between the yrast and yrare bands built on the $\pi h_{11/2} \times \nu h_{11/2}$ configuration. In fact, in the absence of triaxiality, the two bands would not cross, but exhibit a constant energy shift, contrary to experimental evidence.

The collective structure of the yrast band is basically built on the ground-state band of the triaxial core, while the collective structure of the yrare band is predominantly based on the γ band of the core. This finding is at variance with the interpretation of the two bands as a chiral doublet and is further corroborated by the predicted in-band electromagnetic transitions, which have different trends in our interpretation, since the two bands have different structure, while they would have similar trends, if the bands constituted a chiral doublet.

A constant energy spacing between the two lowest positive-parity bands is predicted in other odd-odd $N = 75$ nuclei with γ -soft potential energy surfaces.

Spreading width of the giant dipole resonance at finite temperature

The quasiparticle-phonon model extended to finite nuclear temperature within the framework of thermo-field dynamics has been applied to the calculation of various features of the giant dipole resonance at finite temperature in magic and semi-magic nuclei [A.3].

In particular, the centroid of the E1 strength function turns out to be independent of temperature in the case of the magic nucleus ^{208}Pb and weakly dependent on it in the case of the semi-magic nucleus ^{120}Sn . The same kind of result is obtained for the energy-weighted sum rule.

The most interesting finding is the increase with temperature of the spreading width, Γ_s , defined as the variance of the theoretical E1 strength function, consistent with the experimental trend, shown in Figure 2 for ^{120}Sn and in Figure 3 for ^{208}Pb .

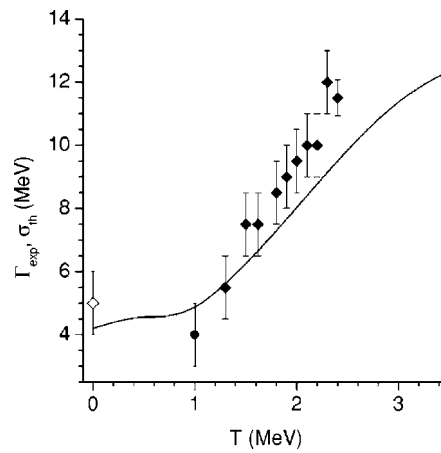


Fig. 2. Temperature dependence of the variance of the theoretical E1 strength function, σ_{th} , and of the experimental width, Γ_{exp} , of the giant dipole resonance in ^{120}Sn . Full diamonds: experimental data revised by D. Kusnezov *et al.*, Phys. Rev. Lett. **81**, 542 (1998); full circle: P. Heckman *et al.*, Phys. Lett. B **555**, 43 (2003); open diamond: T. Baumann *et al.*, Nucl. Phys. A **635**, 428 (1998).

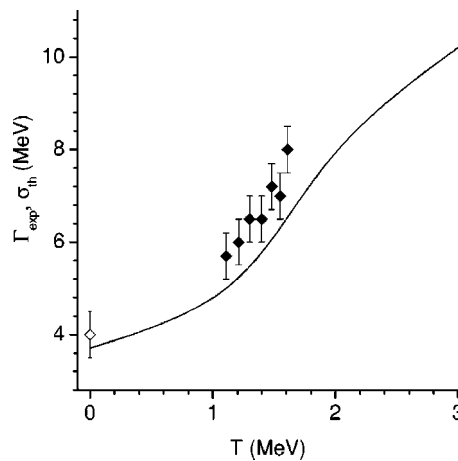


Fig. 3. The same as Fig. 2, but for ^{208}Pb .

The main reason for the increase of the theoretical spreading width with temperature is the coupling of the giant dipole resonance to non-collective thermal phonons of particle-particle, or hole-hole type.

Nuclear Reaction Theory and Experiments

Charge changing interactions of ultra-relativistic Pb nuclei

Within the framework of an international collaboration [A.4], experimental and theoretical results have been obtained on charge loss ($-27 \leq \Delta Z \leq -1$), charge pickup ($\Delta Z = +1$), and total charge changing cross sections for 158A GeV ^{208}Pb ions on CH_2 , C, Al, Cu, Sn and Au targets.

Calculations based on the revisited abrasion-ablation model for hadronic interactions and the relativistic electromagnetic dissociation (RELDIS) model for electromagnetic interactions describe the data in a satisfactory way.

The decay of excited nuclear systems created in both types of interaction is described by the statistical multi-fragmentation model, which includes evaporation, fission and multi-fragmentation channels. At very high projectile energy, the excitation energy of residual nuclei may be estimated on average of the order of 40 MeV per removed nucleon, with a significant increase in comparison with fragmentation of heavy ions of intermediate energy ($\sim 1\text{A GeV}$).

Figure 4 shows a comparison of experimental and theoretical inclusive cross sections for producing a fragment of given charge, Z , by 158A GeV Pb ions on various targets.

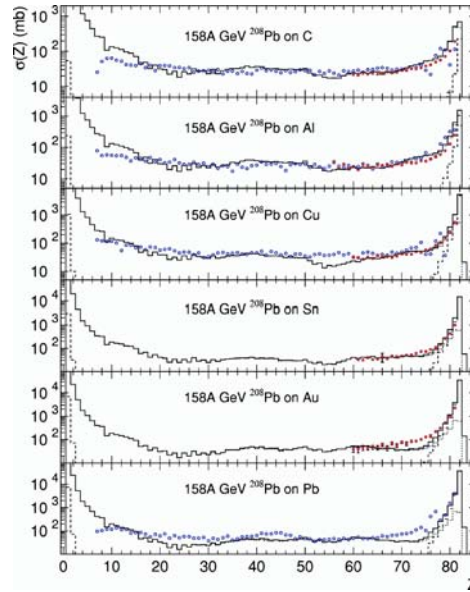


Fig. 4. Inclusive cross sections for producing a fragment with charge Z by 158A GeV ^{208}Pb ions on C, Al, Cu, Sn, Au and Pb targets. Results of the calculations with the abrasion-ablation model and with the RELDIS model are shown by the dotted and dashed histograms, respectively. The solid histograms represent their sums.

A strong increase of nuclear-charge pickup cross sections, forming $_{83}\text{Bi}$, is observed in comparison with similar measurements at 10.6A GeV and is shown in Figure 5. This process is attributed to the electromagnetic production of a negative pion by an equivalent photon and is quantitatively described by the RELDIS model.

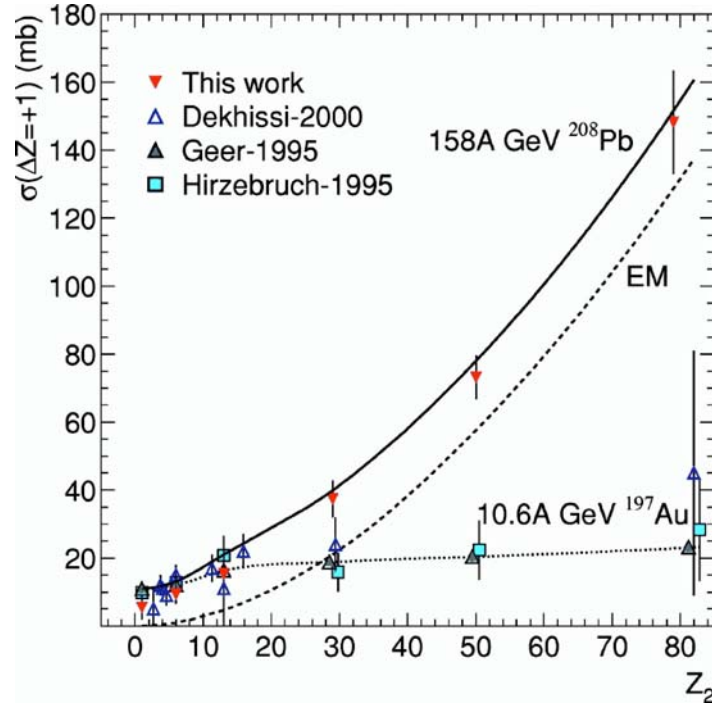


Fig. 5. Nuclear-charge pickup ($\Delta Z = +1$) cross sections as a function of target atomic number, Z_2 . The data for 158A GeV Pb ions are shown by the full (present work) and open triangles (H. Dekhissi *et al.*, Nucl. Phys. A **662**, 207 (2000)). The solid curve is the sum of the electromagnetic contribution (EM, dashed line) and the nuclear contribution to the $\Delta Z = +1$ cross section. For comparison, data obtained with 10.6A GeV Au ions are depicted with the light-colored triangles and squares, connected by the dotted line to guide the eye.

Measurements of neutron cross sections at the n_TOF facility at CERN

The year 2004 saw the conclusion of the campaign of neutron cross-section measurements at the neutron time-of-flight (n_TOF) facility at CERN, exploiting the high instantaneous neutron flux produced on a solid lead target surrounded by a water moderator by spallation induced by the 20 GeV proton beam of the CERN PS accelerator. 135 researchers from 37 institutes were involved in the n_TOF Collaboration.

Purpose of the experimental campaign was to determine with an unprecedented accuracy neutron cross sections of isotopes of interest to nuclear astrophysics (capture) and to accelerator driven systems for nuclear waste transmutation (capture, fission, $(n, 2n)$ and $(n, 3n)$).

Researchers of the ENEA project staff participated in experimental activity (A. Mengoni), theoretical activity (A. Mengoni, A. Ventura) and Monte Carlo simulations (M. Rosetti). Moreover, one of them (A. Mengoni) acted as the coordinator of the n_TOF Collaboration towards the Research Directorate General of the European Commission, who partially financed the activity in the Fifth Framework Programme.

Monte Carlo simulations of the radiation transport in the CERN n_TOF target assembly were performed in order to optimise the spallation target design. The full cascade initiated by the 20 GeV proton beam extracted from the PS accelerator was simulated. The effect of the substitution of the light water moderator with heavy water was assessed. The simulations have shown that this substitution reduces considerably the gamma background (see Fig. 6a-b) without compromising energy resolution and neutron flux. Tritium production in the heavy

water moderator was calculated as well and turned out to be $1.6 \cdot 10^6$ nuclei/cm³/pulse. The simulations were performed by means of the Monte Carlo codes MCNPX and FLUKA.

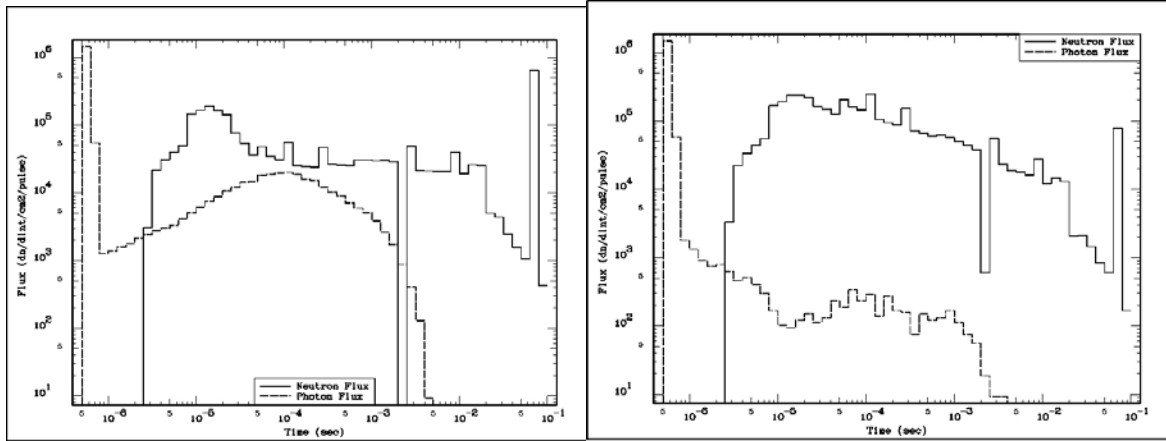


Fig.6a Neutron and photon flux vs. time of arrival at the experimental area for a **light water** moderator.

Fig.6b Neutron and photon flux vs. time of arrival at the experimental area for a **heavy water** moderator.

The papers published in 2004 were focused on instrumentation and techniques of measurement of capture cross sections [A.5-9]. In particular, during the first phase of the project, measurements of (n, γ) cross sections were performed with an array of C₆D₆ liquid scintillators cells, which have the advantage of being among the least sensitive to scattered neutrons [A.5].

The quantity determined in a neutron capture experiment is the capture yield, *i. e.* the fraction of neutrons incident on a sample and undergoing the (n, γ) interaction. Its experimental determination requires the simultaneous measurement of the neutron fluence for normalization. To this end, a low-mass flux monitor was constructed [A.8].

Due to the small solid angle coverage and the low intrinsic efficiency of C₆D₆ detectors, only one γ -ray per event is detected from the de-excitation cascade following neutron capture. For accurate cross-section measurements, the efficiency of the set-up had to be made independent of the details of the de-excitation cascade, in particular of the γ -ray multiplicity. To this end, a pulse height weighting function technique was used and validated by measuring isotopes with well-known resonance capture cross sections, such as ³²S, ¹⁹³Ir and ²³⁸U [A.6]. In particular, the measurements of the 1.298 eV resonance in the ¹⁹³Ir (n, γ) cross section indicated that this standard needs to be revised to a value of 1.3047 ± 0.0003 eV [A.9].

The first physical result published by the Collaboration is the (n, γ) cross section of ¹⁵¹Sm in the energy range from 1 eV to 1 MeV [A.10], which is of importance for characterizing neutron capture nucleosynthesis in asymptotic giant branch stars. Resolved resonances up to $E_n = 400$ eV were detected, thus providing a new accurate *s*-wave resonance spacing, $D_0 = 1.48 \pm 0.04$ eV. Figure 7 shows their cumulative number as a function of E_n

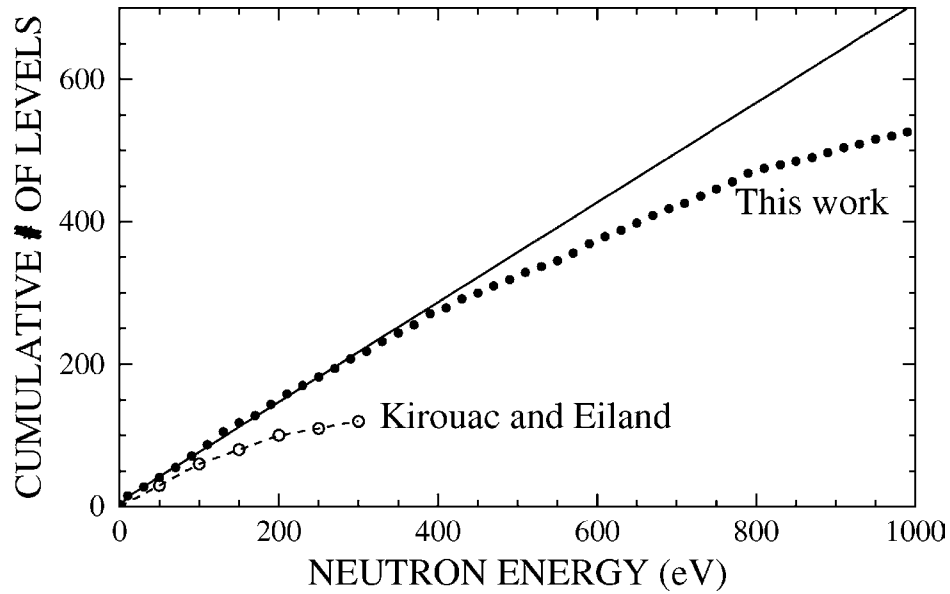


Fig.7. Cumulative number of levels at the neutron separation energy of ^{152}Sm fitted at energies below 40 eV, in comparison with the measurements of G. Kirouac and H. Eiland, Phys. Rev. C **11**, 895 (1975).

At the thermal energy of $kT = 30 \text{ KeV}$, the Maxwellian averaged cross section was determined to be $3100 \pm 160 \text{ mb}$, significantly larger than theoretical predictions.

Preliminary results on experimental methods and cross-section measurements were presented at the 8th International Symposium on Nuclei in the Cosmos, Vancouver, Canada, 19-23 July 2004 [C.1-3] and at the International Conference on Nuclear Data for Science and Technology, Santa Fe, New Mexico, USA, 26 September-01 October 2004 [C.4-10].

A work closely connected with theoretical activities in the frame of the n_TOF Collaboration is the new version (Lodi) of the nuclear reaction model code Empire-2: the new developments include an improved fission channel with multiple-humped barrier penetrabilities for low-energy fission, pre-equilibrium emission of composite particles, such as deuterons, tritons and alphas, photo-nuclear reactions and reactions on excited targets [C.11].

Neutron capture cross section of ^{135}Cs

The neutron capture cross section of the unstable isotope ^{135}Cs was measured relative to that of gold by means of the activation method. The neutron capture cross sections were determined at $E_n = 30 \text{ keV}$ and 500 keV , as shown in Figure 8, and were used to normalize the theoretically derived cross-section shape. Based on these data, statistical model calculations were performed to obtain the capture cross sections of the short-lived isotopes ^{134}Cs and ^{136}Cs as well.

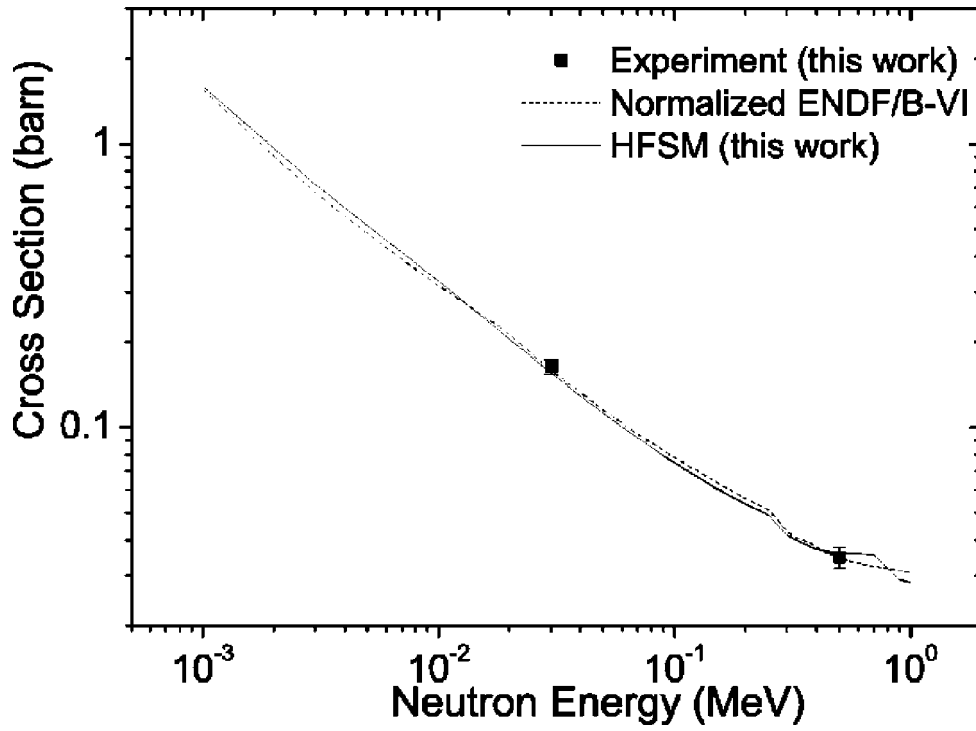


Fig.8. Experimental and evaluated results for the $^{135}\text{Cs}(n,\gamma)^{136}\text{Cs}$ cross section. The evaluated data have been normalized to the experimental points.

Updated Maxwellian-averaged capture cross sections of all unstable Cs isotopes were calculated for a range of thermal energies characteristic of helium burning scenarios for an improved *s*-process analysis of the Xe-Cs-Ba region [A.11].

Neutron capture cross sections of ^{208}Pb and ^{209}Bi

Stellar cross sections of importance with respect to the termination of the *s*-process reaction chain were determined for $^{208}\text{Pb}(n,\gamma)^{209}\text{Pb}$ and $^{209}\text{Bi}(n,\gamma)^{210}\text{Bi}^g$, yielding $kT = 30$ keV values of $\langle\sigma v\rangle/v_T = 0.31 \pm 0.2$ mb and 2.54 ± 0.14 mb, respectively [A.12].

The measurements were carried out by activation of Pb and Bi samples in a quasistellar neutron spectrum using gold as a cross-section standard. With this technique the uncertainties reported in previous works could be considerably reduced.

The measurements were complemented by a discussion of the recycling at the termination point of the *s*-process neutron capture chain in a 3-solar-masses and $[\text{Fe}/\text{H}] = -1.3$ asymptotic giant branch star. At this metallicity, AGB stars give rise to the maximum production of *s*-process lead. The sensitivity of the isotopic lead abundances was discussed with respect to the remaining cross-section uncertainties.

The information obtained in this work is also of relevance for an assessment of the α activity due to a buildup of ^{210}Po in Pb/Bi cooled fast reactors.

Coulomb and nuclear breakup of the halo nucleus ^{11}Be

Breakup reactions of the one-neutron halo nucleus ^{11}Be on Pb and C targets at about 70 MeV/nucleon were investigated at RIKEN [A.13]. The relative energy spectra as well as the angular distributions of the $^{10}\text{Be} + n$ centre-of-mass system were extracted both for Pb and C targets.

For the breakup of ^{11}Be on Pb, the selection of forward-scattering angles, corresponding to large impact parameters, was found to be effective to extract almost purely the first-order E1 Coulomb breakup component and to exclude the nuclear component and higher-order Coulomb components. This angle-selected energy spectrum was thus used to deduce the spectroscopic factor for the $^{10}\text{Be}(0^+) \text{ xv } 2s_{1/2}$ configuration in ^{11}Be , which was found to be 0.72 ± 0.04 with a $B(E1)$ strength up to $E_x = 4$ MeV of $1.05 \pm 0.06 \text{ e}^2 \text{ fm}^2$. The energy-weighted E1 strength up to $E_x = 4$ MeV explains $70\% \pm 10\%$ of the cluster sum rule, consistent with the observed spectroscopic factor.

The non-energy-weighted sum rule within the same energy range was used to extract the root-mean-square distance of the halo neutron to be 5.77(16) fm, consistent with previously known values.

In the breakup with the carbon target, the excitations to the known unbound states in ^{11}Be at $E_x = 1.78$ MeV and $E_x = 3.41$ MeV were observed. Angular distributions for these states show the diffraction pattern characteristic of $L = 2$ transitions, resulting in a $J^\pi = (3/2, 5/2)^+$ assignment for these states. It was finally found that even for the C target the E1 Coulomb direct breakup mechanism becomes dominant at very forward angles.

Nuclear Data Processing and Validation

The cooperation of the ENEA Nuclear Data Group with OECD/NEA Data Bank (Issy-les-Moulineaux, France) continued, in particular, within the framework of the activities performed in the JEFF Working Group on Benchmark Testing, Data Processing and Evaluations.

The collaboration with specialists of the Russian research and development Institute of Physics and Power Engineering of Obninsk (IPPE-Obninsk) was continued and extended. The nuclear data processing activity was exclusively dedicated to produce, to test and to report a new large multigroup library in MATXS format, named MATJEF22.BOLIB. Since OECD/NEA Data Bank requested this library, it is foreseen to release MATJEF22.BOLIB to that International Agency for free dissemination.

MATJEF22.BOLIB Multigroup Library

The ENEA-Bologna Nuclear Data Group produced the MATJEF22.BOLIB multigroup coupled neutron and photon cross-section library in MATXS format for nuclear fission applications, based on the JEF-2.2 European nuclear data file. Concerning this, a co-operation with specialists of IPPE-Obninsk was renewed. The present MATJEF22.BOLIB library [R.1] has the same energy group structure (199 neutron groups and 42 photon groups) and general features as the DLC-184/VITAMIN-B6 American library. The production of the

MATJEF22.BOLIB and VITJEF22.BOLIB (NEA-1699 ZZ VITJEF22.BOLIB) libraries, respectively in MATXS and AMPX formats, was conceived in ENEA-Bologna to propose to the users of the JEF-2.2 data file European counterparts of the VITAMIN-B6 library, based on the ENDF/B-VI Release 3 American nuclear data file. In fact the aim was to produce fine-group pseudo-problem-independent libraries based on the Bondarenko (f-factor) method for the treatment of neutron resonance self-shielding and temperature effects. For the pseudo-problem-independent multigroup library it is understood that the library is prepared with sufficient detail in energy, temperatures and resonance self-shielding so as to be applicable to a wide range of physical systems. The same GENDF data files of multigroup cross sections are the basis of the MATJEF22.BOLIB and VITJEF22.BOLIB libraries and they were produced through an automatic calculation procedure, based on the NJOY-94.66 (LANL) nuclear data processing system. In particular this automatic procedure, developed in ENEA-Bologna, permits fast generation of groupwise cross-section libraries in the MATXS or AMPX formats with the potential of producing working libraries, through further proper data processing, respectively with the TRANSX (LANL) code and with the AMPX or SCAMPI (ORNL) systems. In particular, TRANSX can produce broad-group collapsed libraries of self-shielded neutron cross sections for different applications, in the formats used by the deterministic codes included in the DANTSYS (LANL) and DOORS (ORNL) systems while AMPX or SCAMPI give the same possibility for the codes of the DOORS system.

As already introduced, MATJEF22.BOLIB is characterized by the same group structure of VITAMIN-B6 with 199 neutron groups and 42 photon groups and contains at present 138 isotopes/natural elements. In particular 133 nuclides were processed at 4 temperatures (300 °K, 600 °K, 1000 °K and 2100 °K) and up to 10 background cross sections. The cross sections were obtained for the most part with 6 to 8 values for the background cross section to permit a proper interpolation of the self-shielding factors in order to create working libraries. Moreover, thermal scattering cross sections for 5 important moderating elements (H-1 in light water, H-1 in polyethylene, H-2 in heavy water, C in graphite and Be in beryllium metal) were processed through the THERMR and GROUPT modules of NJOY, starting from the corresponding thermal scattering matrices $S(\alpha, \beta)$ at all the temperatures available in the original JEF-2.2 thermal scattering law data file.

It is underlined that the thermal neutron energy range, characterized by those energy groups which include upscatter, contains 36 groups and has 5.043 eV as the uppermost boundary. The order of scattering used for both neutrons and photons is P7 for nuclides with $Z=1$ through $Z=29$ (copper) and P5 for the remainder of the nuclides.

The neutron and photon weighting functions used to produce the MATJEF22.BOLIB library cross sections are the same employed in the generation of the VITAMIN-B6 cross sections. The neutron weighting function is of the form typically chosen for fission reactor shielding problems, i.e., it consists of a smoothly varying combination of a Maxwellian thermal spectrum, a fission spectrum, and a "1/E" slowing down spectrum. This corresponds to a WT = 4 option in the GROUPT module of NJOY. The breakpoint energies for the 3-region spectrum are similar to those used in the VITAMIN-C (ORNL) library. The breakpoint energy between the Maxwellian and 1/E shapes is 0.125 eV. The fission temperature has been adjusted to better reflect the neutron spectrum in a thermal reactor ($\theta = 1.273$ MeV versus $\theta = 1.41$ MeV for the VITAMIN-E (ORNL) library).

Functional Form	Energy Limits	Groups
1. Maxwellian Thermal Spectrum ($kT = 0.025$ eV)		
$W_1(E) = C_1 E e^{-E/kT}$	1.0E-5 eV to 0.125 eV	188-199
2. "1/E" Slowing-Down Spectrum		
$W_2(E) = C_2/E$	0.125 eV to 820.8 keV	167-187
3. Fission Spectrum ($\theta = 1.273$ MeV)		
$W_3(E) = C_3 E^{1/2} e^{-E/\theta}$	820.8 keV to 20 MeV	1-66

A continuous weighting spectrum is achieved with the following constants: $C_1 = 9498.4 \text{ eV}^{-2}$; $C_2 = 1.0$; and $C_3 = 2.5625 \text{ MeV}^{-1.5}$.

The photon weighting spectrum consists of a 1/E spectrum with a "roll-off" of the spectrum at lower energies to represent photoelectric absorption and a similar drop-off of the spectrum at higher energies corresponding to the Q-value for neutron capture. This corresponds to the IWT = 3 input option in the GAMINR module of NJOY.

In general, it was considered important to update and to extend the availability of multigroup cross-section libraries for computer simulations of nuclear fission systems with discrete ordinates codes. It is underlined that the main intention was to offer to the users of 3D deterministic codes, like TORT (ORNL) and THREEDANT (LANL), the possibility to generate working cross-section libraries based on JEF-2.2 European data. This with the main perspective of increasing the power of application of the modern multi-dimensional discrete ordinates deterministic codes which can continue to offer important complementary information with respect to the results obtained with the Monte Carlo codes. It is believed, in fact, that the availability of rigorous analytical solutions of the neutral particle transport problems represents an objective important value in all possible applications.

It is expected that the multi-purpose nature of MATJEF22.BOLIB and VITJEF22.BOLIB, like the VITAMIN-B6 library, will make these ENEA-Bologna libraries useful for shielding applications and potentially for reactor physics analyses.

Computer Codes

BOT3P Code Package Development

BOT3P consists of a set of standard FORTRAN 77 language programs developed at the ENEA-Bologna Nuclear Data Group. BOT3P was originally conceived to give the users of the DORT and TORT deterministic transport codes some useful diagnostic tools to prepare and to check their input data files. Later BOT3P versions [A.14] introduced some important additions in the input geometrical model description and extended the possibility to produce the geometrical, material distribution and fixed neutron source data to the deterministic transport codes TWODANT, THREEDANT and PARTISN, and in case of X-Y-Z mesh

grids, a geometrical input to the MCNP Monte Carlo transport code, starting from the same input to BOT3P.

Versions from BOT3P 4.0 [R.2, R.3] up to BOT3P 4.2 [R.4] were developed in 2004. They extend the modelling capabilities of previous BOT3P versions, reduce CPU times and facilitate the debugging of the computer code input. The geometrical entries for the sensitivity code SUS3D are also produced, for both Cartesian and cylindrical geometries and the fine mesh arrays and the material zone map are stored in a binary file, the content of which can be visualized by the graphics' modules of BOT3P. This new feature makes interfacing to any deterministic and Monte Carlo transport code easy and might open new promising application fields to this package.

Through the use of BOT3P, radiation transport problems with complex 3D geometrical structures can be modelled easily, as a relatively small amount of engineer-time is required and refinement is achieved by changing few parameters. This tool is useful for solving very large challenging problems.

BOT3P was developed on a DIGITAL UNIX ALPHA 500/333 Workstation and successfully used in some complex neutron shielding and criticality benchmarks. It was also tested on Red Hat Linux 7.1 and is designed to run on most UNIX platforms.

All BOT3P versions are publicly available from the Organization for Economic Cooperation and Development/Nuclear Energy Agency (OECD/NEA) Data Bank [CC1].

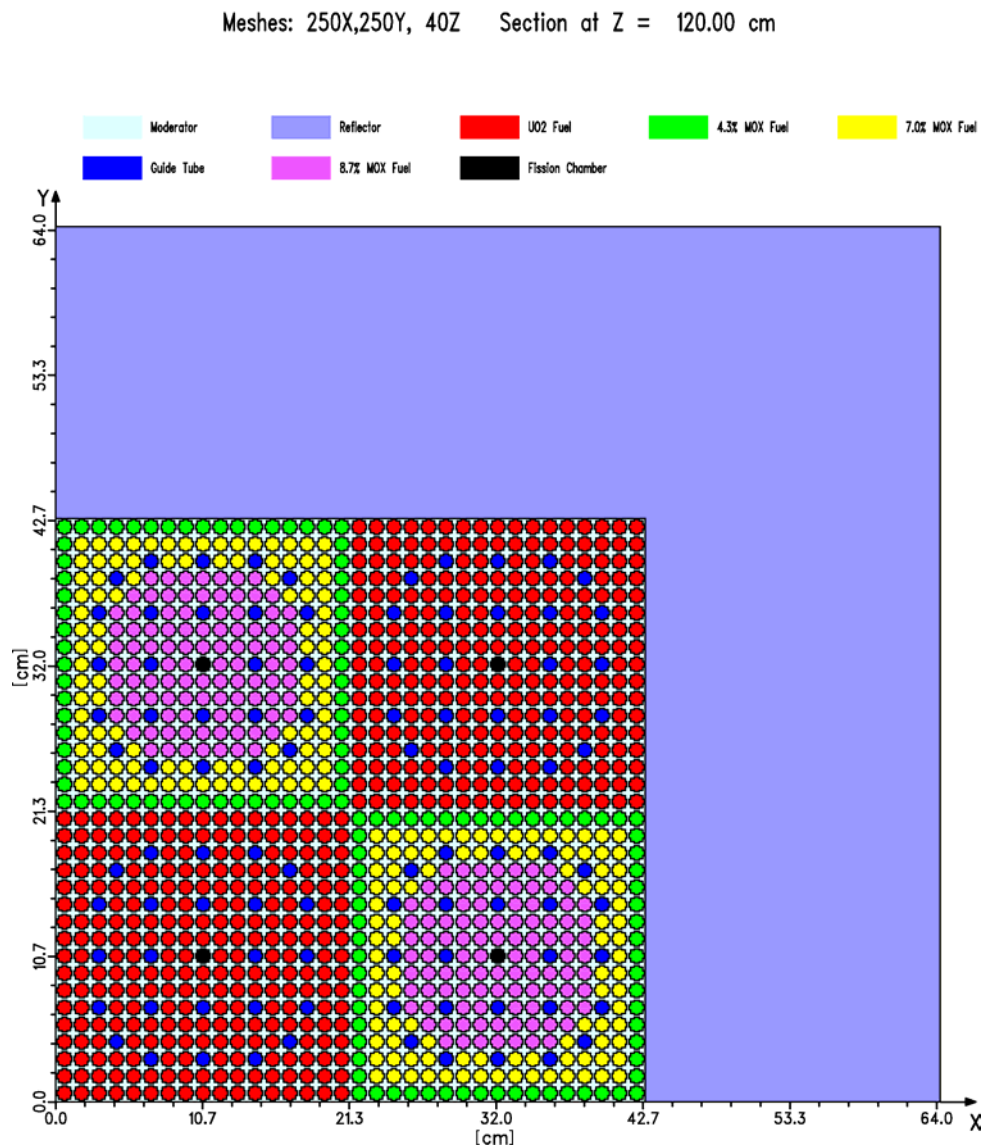
The following programs are included in the BOT3P software package: GGDM, DDM, GGTM, DTM2, DTM3, RVARSL, COMPARE and MKSRC. In particular:

- GGDM generates the geometry and material entries for DORT, TWODANT, PARTISN and SUS3D and for other potential 2D transport codes through its output binary file.
- GGTM generates the geometry and material entries for TORT, THREEDANT, PARTISN, SUS3D and other potential 3D transport codes through its output binary file, and, only in case of X-Y-Z geometry, for MCNP.
- DDM is a graphics pre/post-processor for DORT/TWODANT/PARTISN configuration or computed field.
- DTM2 is a 2D graphics pre/post-processor for TORT, THREEDANT, PARTISN configuration or computed field.
- DTM3 is a 3D graphics pre/post-processor for TORT, THREEDANT, PARTISN configuration or computed field.
- RVARSL reads DORT/TORT VARSL-format output files or the standard interface RTFLUX files generated by TWODANT/THREEDANT/PARTISN (feature introduced by Dr. A. Bidaud, Institut de Physique Nucleaire Orsay, France) and then prepares output for post-processing.
- COMPARE, also contributed by Dr. A. Bidaud, calculates the ratio between the same target quantity obtained in two different transport analyses on the same mesh grid for further plot with one of the BOT3P graphics programs.
- MKSRC writes a general neutron input source in format varsl for DORT, flxmom for TORT and fixsrc for TWODANT/THREEDANT/PARTISN.

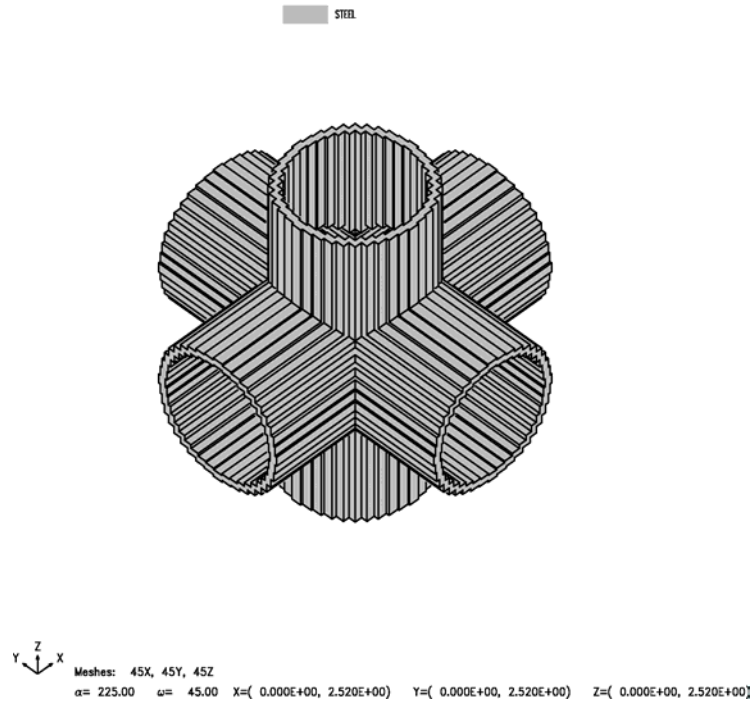
DDM and DTM2/DTM3 may be linked to any 2D and 3D transport code respectively, if proper interfaces to manage DDM/DTM2/DTM3 binary input/output files have been arranged.

The following three plots are examples of the BOT3P complex modelling capabilities. The first one refers to the C5G7MOX Benchmark Problem [A.15], the second one shows three mutual orthogonal pipes of the same radius where volume is preserved. The third plot shows the core region and the steel zones of the R- Θ -Z model used in the ENEA Bologna VENUS-3 (<http://www.nea.fr/html/science/shielding/sinbad/venus3/ven3-abs.htm>) neutron shielding benchmark calculations.

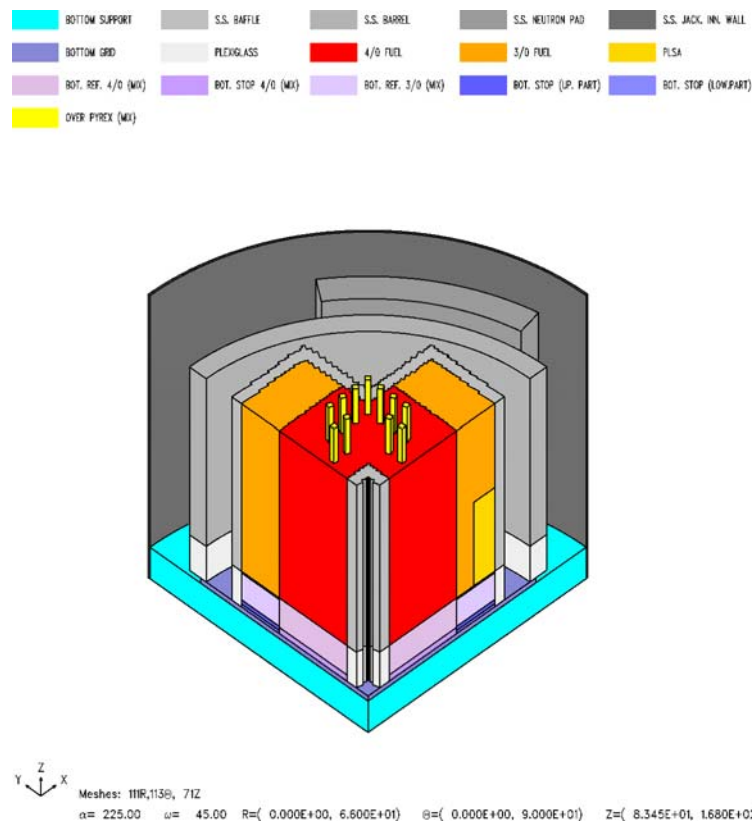
Lewis MOX Fuel Assembly Benchmark (XYZ TORT Model with Material Borders plotted)



Three Mutual Orthogonal Pipes with the Same Radius



VENUS-3 Benchmark. 3D View of Core Region and Steel Zones (RØZ TORT Model)



ENEA Bologna has given a consulting support to the Nuclear Division of ANSALDO Energia SpA to use BOT3P Version 4.1 in order to produce a detailed R- Θ -Z geometrical model for their TORT calculations on components of a 1000 MW PWR nuclear power reactor and to visualize and process the related computed field.

ADEFTA Version 2.0 Development

ADEFTA (Atomic Densities for Transport Analysis) [CC.2] is a script file for any UNIX/Linux platform that uses only Bourne shell (bash) commands and the “awk” UNIX (and Linux) utility in order to calculate the atomic densities related to any compositional model for transport analysis. Moreover ADEFTA is particularly addressed to users of both the GIP code, which prepares macroscopic cross sections for the DORT/TORT deterministic transport codes, and the Monte-Carlo code MCNP.

Version 2.0 [R.5], differently from Version 1.0, accepts to input the isotopic concentration of isotopes or natural elements in a material definition also. This option is useful when the isotopic concentration of a medium is a problem input, because already calculated elsewhere. ADEFTA calculates the concentration of isotopes resulting from the "splitting" of natural elements (when necessary) and uses these input and/or calculated isotopic concentrations to determine the isotopic concentrations of mixtures, if any.

ADEFTA is publicly available from the Organization for Economic Cooperation and Development/Nuclear Energy Agency (OECD/NEA) Data Bank [CC.2].

Publications

Articles

- [A.1] G. Lévai, F. Cannata and A. Ventura, *The interplay of different symmetries in quantum mechanical potentials*, Acta Phys. Hung. NS-H 19, 281 (2004).
- [A.2] S. Brant, D. Vretenar and A. Ventura, *Interacting boson fermion-fermion model calculation of the $\pi h_{11/2} \times \nu h_{11/2}$ doublet bands in ^{134}Pr* , Phys. Rev. C **69**, 017304 (2004).
- [A.3] A. N. Storozhenko, A. I. Vdovin, A. Ventura and A. I. Blokhin, *Temperature dependence of spreading width of giant dipole resonance*, Phys. Rev. C **69**, 064320 (2004).
- [A.4] C. Scheidenberger, I. A. Pshenichnov, K. Sümmerer, A. Ventura, J. P. Bondorf, A. S. Botvina, I. N. Mishustin, D. Boutin, S. Datz, H. Geissel, P. Grafström, H. Knudsen, H. F. Krause, B. Lommel, S. P. Möller, G. Münzenberg, R. H. Schuch, E. Uggerhøj, U. Uggerhøj, C R. Vane, Z. Z. Vilakazi and H. Weick, *Charge-changing interactions of ultrarelativistic Pb nuclei*, Phys. Rev. C **70**, 014902 (2004).

- [A.5] P. M. Milazzo, G. Aerts, E. Berthomieux, N. Bustreo, D. Cano-Ott, P. Cennini, N. Colonna, C. Domingo, M. Embid, L. Ferrant, E. Gonzales, F. Gunsing, M. Heil, F. Käppeler, S. Marrone, P. F. Mastinu, A. Mengoni, C. Moreau, J. Pancin, T. Papaevangelou, C. Paradela, P. Pavlopoulos, R. Plag, R. Reifarh, C. Stephan, L. Tassan-Got, G. Tagliente, J. L. Tain, R. Terlizzi and V. Vlachoudis, *Measurements of neutron capture cross sections for ADS-related studies*, Nucl. Instrum. Meth. Phys. Res. B **213**, 36 (2004).
- [A.6] The n_TOF Collaboration : U. Abbondanno, G. Aerts, H. Alvarez, S. Andriamonje, A. Angelopoulos, P. Assimakopoulos, C. O. Bacri, G. Badurek, P. Baumann, F. Bečvář, H. Beer, J. Benlliure, B. Berthier, E. Berthomieux, S. Boffi, C. Borcea, E. Boscolo- Marchi, N. Bustreo, P. Calviño, D. Cano-Ott, R. Capote, P. Carlson, P. Cennini, V. Chepel, E. Chiaveri, C. Coceva, N. Colonna, G. Cortes, D. Cortina, A. Couture, J. Cox, S. Dababneh, M. Dahlfors, S. David, R. Dolfini, C. Domingo-Pardo, I. Duran, C. Eleftheriadis, M. Embid-Segura, L. Ferrant, A. Ferrari, L. Ferreira-Lourenco, R. Ferreira-Marques, H. Fraiss-Koelbl, W. I. Furman, Y. Giomataris, I. F. Goncalves, E. Gonzalez-Romero, A. Goverdovski, F. Gramegna, E. Griesmayer, F. Gunsing, R. Haight, M. Heil, A. Herrera-Martinez, K. G. Ioannides, N. Janeva, E. Jericha, F. Käppeler, Y. Kadi, D. Karamanis, A. Kelic, V. Ketlerov, G. Kitis, P. E. Koehler, V. Konovalov, E. Kosionides, V. Lacoste, H. Leeb, A. Lindote, M. I. Lopes, M. Lozano, Lukic, S. Markov, S. Marrone, J. Martinez-Val, P. F. Mastinu, A. Mengoni, P. M. Milazzo, E. Minguez, A. Molina-Coballes, C. Moreau, F. Neves, H. Oberhummer, S. O' Brien, J. Pancin, T. Papaevangelou, C. Paradela, A. Pavlik, P. Pavlopoulos, A. Perez-Parra, J. M. Perlado, L. Perrot, V. Peskov, R. Plag, A. Plompen, A. Plukis, A. Poch, A. Policarpo, C. Pretel, J. M. Quesada, M. Radici, S. Raman, W. Rapp, T. Rauscher, R. Reifarh, F. Rejmund, M. Rosetti, C. Rubbia, G. Rudolf, P. Rullhusen, J. Salgado, E. Savvidis, J. C. Soares, C. Stephan, G. Tagliente, J. L. Tain, C. Tapia, L. Tassan-Got, L. M. N. Tavora, R. Terlizzi, M. Terrani, N. Tsangas, G. Vannini, P. Vaz, A. Ventura, D. Villamarin-Fernandez, M. Vincente-Vincente, V. Vlachoudis, R. Vlastou, F. Voss, H. Wendler, M. Wiescher, K. Wisshak and L. Zanini: *New experimental validation of the pulse height weighting technique for capture cross-section measurements*, Nucl. Instrum. Meth. Phys. Res. A **521**, 454 (2004).
- [A.7] J. Pancin and the n_TOF Collaboration: *Measurement of the n_TOF beam profile with a micromegas detector*, Nucl. Instrum. Meth. Phys. Res. A **524**, 102 (2004).
- [A.8] P. F. Mastinu and the n_TOF Collaboration: *A low-mass neutron flux monitor for the n_TOF facility at CERN*, Braz. J. Phys. **34**, 914 (2004).
- [A.9] G. Lorusso and the n_TOF Collaboration: *Time-energy relation of the n_TOF neutron energy beam: energy standards revisited*, Nucl. Instrum. Meth. Phys. Res. A **532**, 622 (2004).
- [A.10] The n_TOF Collaboration: *Neutron capture cross-section measurement of ^{151}Sm at the CERN neutron time of flight facility (n_TOF)*, Phys. Rev. Lett. **93**, 161103 (2004).
- [A.11] N. Patronis, S. Dababneh, P. A. Assimakopoulos, R. Gallino, M. Heil, F. Käppeler, D. Karamanis, P. E. Koehler, A. Mengoni and R. Plag, *Neutron capture studies on unstable ^{135}Cs for nucleosynthesis and transmutation*, Phys. Rev. C **69**, 025803 (2004).
- [A.12] U. Ratzel, C. Arlandini, F. Käppeler, A. Couture, M. Wiescher, R. Reifarh, R. Gallino, A. Mengoni and C. Travaglio, *Nucleosynthesis at the termination point of the s-process*, Phys. Rev. C **70**, 065803 (2004).

- [A.13] N. Fukuda, T. Nakamura, N. Aoi, N. Imai, M. Ishihara, T. Kobayashi, H. Iwasaki, T. Kubo, A. Mengoni, M. Notani, H. Otsu, H. Sakurai, S. Shimoura, T. Teranishi, Y. X. Watanabe and K. Yoneda, *Coulomb and nuclear breakup of a halo nucleus ^{11}Be* , Phys. Rev. C **70**, 054606 (2004).
- [A.14] R. Orsi, *BOT3P: Bologna Transport Analysis Pre-Post-Processors Version 3.0*, Nucl. Sci. Eng. **146**, 248 (2004).
- [A.15] Y. Y. Azmy, J. C. Gehin, R. Orsi, *DORT Solutions to the Two-Dimensional C5G7MOX Benchmark Problem*, Progr. Nucl. Energy **45**, 215 (2004).

Conference Contributions

- [C.1] The n_TOF Collaboration: *Neutron capture cross-section measurements for nuclear astrophysics at CERN n_TOF*, 8th Int. Symp. on Nuclei in the Cosmos, Vancouver, July 19-23, 2004 (to be published in a special issue of Nucl. Phys. A).
- [C.2] The n_TOF Collaboration: *Measurement of the $^{151}\text{Sm}(n,\gamma)^{152}\text{Sm}$ cross section at n_TOF*, 8th Int. Symp. on Nuclei in the Cosmos, Vancouver, July 19-23, 2004 (to be published in a special issue of Nucl. Phys. A).
- [C.3] G. Tagliente and the n_TOF Collaboration: *Measurements of the $^{90,91,92,94,96}\text{Zr}(n,\gamma)$ cross sections at n_TOF*, 8th Int. Symp. on Nuclei in the Cosmos, Vancouver, July 19-23, 2004 (to be published in a special issue of Nucl. Phys. A).
- [C.4] The n_TOF Collaboration: *The n_TOF facility at CERN: performances and first physical results*, Int. Conf. on Nuclear Data for Science and Technology, Santa Fe, 26 September-01 October 2004.
- [C.5] C. Moreau and the n_TOF Collaboration: *Measurements of capture cross sections of $^{90,91,92,94,96}\text{Zr}$ at CERN n_TOF*, Int. Conf. on Nuclear Data for Science and Technology, Santa Fe, 26 September-01 October 2004.
- [C.6] C. Domingo-Pardo and the n_TOF Collaboration: *New measurement of capture cross sections of bismuth and lead*, Int. Conf. on Nuclear Data for Science and Technology, Santa Fe, 26 September-01 October 2004.
- [C.7] M. Mosconi and the n_TOF Collaboration: *Neutron capture cross sections for the Re/Os clock*, Int. Conf. on Nuclear Data for Science and Technology, Santa Fe, 26 September-01 October 2004.
- [C.8] G. Aerts and the n_TOF Collaboration: *Measurement of the ^{232}Th capture cross section at the CERN n_TOF facility*, Int. Conf. on Nuclear Data for Science and Technology, Santa Fe, 26 September-01 October 2004.
- [C.9] D. Cano-Ott and the n_TOF Collaboration: *Measurements at n_TOF of the capture cross sections of minor actinides relevant to nuclear waste transmutation*, Int. Conf. on Nuclear Data for Science and Technology, Santa Fe, 26 September-01 October 2004.
- [C.10] W. Furman and the n_TOF Collaboration: *High resolution study of the ^{237}Np fission cross section from 5 eV to 1 MeV*, Int. Conf. on Nuclear Data for Science and Technology, Santa Fe, 26 September-01 October 2004.
- [C.11] M. Herman, P. Obložinsky, R. Capote, M. Sin, A. Trkov, A. Ventura and V. Zerkin, *Recent developments of the nuclear reaction model code Empire*, Int. Conf. on Nuclear Data for Science and Technology, Santa Fe, 26 September-01 October 2004.
- [C.12] J. J. Klingensmith, Y. Y. Azmy, J. C. Gehin, R. Orsi. *TORT Solutions to the Three-Dimensional MOX Neutron Transport Benchmark Problem, 3-D Extension C5G7 MOX*, Conference PHISOR-2004: (The Physics of Fuel Cycles and Advanced Nuclear Systems: Global Developments), Chicago, 25-29 April 2004.

Reports

- [R.1] M. Pescarini, R. Orsi, T. Martinelli, A.I. Blokhin, V. Sinitsa, *MATJEF22.BOLIB – A JEF-2.2 Multigroup Coupled (199 n + 42 γ) Cross-section Library in MATXS Format for Nuclear Fission Applications*, ENEA/FIS –P815-007, June 6, 2004.
- [R.2] R. Orsi, BOT3P Version 4.0: *The ENEA Bologna Pre/Post-Processors of the DORT, TORT TWODANT, THREEDANT Transport Codes*, ENEA/FIS-P815-008 Rev.0, August 5, 2004.
- [R.3] R. Orsi, BOT3P Version 4.0: *The ENEA Bologna Pre/Post-Processors of the DORT, TORT, WODANT, THREEDANT Transport Codes*, ENEA/FIS-P815-008 Rev.1, November 2, 2004.
- [R.4] R. Orsi, BOT3P Version 4.2: *The ENEA Bologna Pre/Post-Processors of the DORT, TORT, TWODANT, THREEDANT Transport Codes*, ENEA/FIS-P815-008 Rev.0, Dec. 20, 2004.
- [R.5] R. Orsi, ADEFTA Version 2.0: *A Program to Calculate the Atomic Densities of a compositional Model for Transport Analysis*, ENEA/FIS-P9H6-001 Rev.0, Nov. 8, 2004.

Computer Codes

- [CC.1] R. Orsi, NEA-1678/05 BOT3P4.1. BOT3P4.1, *3D Mesh Generator and Graphical Display of Geometry for Radiation Transport Codes, Display of Results*, Organization for Cooperation and Development Nuclear Energy Agency Data Bank, Issy-les-Moulineaux, France (<http://www.nea.fr/abs/html/nea-1678.html>), 2004.
- [CC.2] R. Orsi, NEA-1708 ADEFTA 2.0. ADEFTA 2.0, *Atomic Densities for Transport Analysis*, Organization for Economic Cooperation and Development Nuclear Energy Agency Data Bank, Issy-les-Moulineaux, France (<http://www.nea.fr/abs/html/nea-1708.html>), 2004.

Project Staff

Mr. Tiziano Martinelli
Dr. Alberto Mengoni
Dr. Roberto Orsi
Dr. Massimo Pescarini
Dr. Maurizio Rosetti (part-time)
Dr. Alberto Ventura

Visiting Scientists

Prof. Slobodan Brant,
Department of Physics,
Faculty of Science,
University of Zagreb, Croatia
(February 2004)

Dr. Anatoly I. Blokhin
Institute of Physics and Power Engineering
Obninsk, Kaluga Region,
Russian Federation
(January – March 2004)

Nuclear Data Section
International Atomic Energy Agency
P.O. Box 100
A-1400 Vienna
Austria

e-mail: services@iaecand.iaea.org
fax: (43-1) 26007
cable: INATOM VIENNA
telex: 1-12645
telephone: (43-1) 2600-21710